Journal of Theoretical and Applied Physics (JTAP), Vol.15, No. 1, 152104 (1-6), 2021
Received 23 September 2021; Accepted 13 November 2021; [http://dx.doi.org/1030495/jtap.152104]

Detection of mercaptopurine drug by T4,4,4-graphyne and the effect of applied electric field: A density functional theory study

Roya Majidi[1]*

Abstract
In the present work, adsorption of mercaptopurine (MP) drug on T4,4,4-graphyne sheet is examined by using density functional theory to explore the feasibility of T4,4,4-graphyne based sensor. The most stable configuration, charge transfer, adsorption energy, electronic band structures, and density of states are determined. It is found that weak physical adsorption with small charge transfer from T4,4,4-graphyne to MP drug took place. T4,4,4-graphyne sheet is an intrinsic semiconductor with a direct band gap. The energy band gap of T4,4,4-graphyne sheet is sensitive to the MP adsorption and decreases with any decrease in the concentration of the MP drug. Hence, T4,4,4-graphyne is a good candidate to detect the MP drug and its concentration. The electronic properties of T4,4,4-graphyne sheet with adsorbed MP are remarkably modulated by applying a perpendicular electric field. The results reveal that applying the electric field is a helpful method to improve the sensing performance of T4,4,4-graphyne sheet.

Keywords
graphyne, energy band gap, sensing property, electronic properties, first principle study.

[1] *Department of Physics, Shahid Rajaee Teacher Training University, Lavizan, 16788-15811 Tehran, Iran*
*__Corresponding author__: royamajidi@gmail.com

1. Introduction

Mercaptopurine (MP) is an anticancer chemotherapy drug utilized to treat acute lymphocytic leukemia, ulcerative colitis, and Crohn's disease [1–3]. It is an immunosuppressive drug with common side effects including liver toxicity, vomiting, loss of appetite, and bone marrow suppression [1–3]. Traditionally, this drug was not suggested for pregnant women because early evidence indicated that receiving MP within the first trimester of pregnancy increases the incidence of abortion and the overall rate of congenital malformations [4]. However, more recent and larger studies reported that the use of the MP drug does not increase fetal malformations [3–5]. Unfortunately, this drug has the possible risk to cause cancer in humans, and using large doses of MP with other cytotoxic drugs increases the risk of developing leukemia [6]. For this reason, safe, simple, reliable, fast response, and economical sensors are highly required. Nowadays, many approaches such as capillary electrophoresis, high performance liquid chromatography, fluorescence, spectrophotometric, and electrochemical have been used to find MP drug in the blood or biological fluids [7–12]. The complicated procedure, long response time, high cost, and low detection capability are the main disadvantages of these methods [1, 3]. Nanotechnology provides significant advances to overcome the limitations of conventional materials. A novel sensor group with low cost and high sensitivity has been provided based on nanostructures [1–3, 13–18]. The carbon-based low dimensional structures including fullerenes, carbon nanotubes, and graphene are the most studied and currently used nanomaterials because of their special structures and remarkable properties. Fullerene is a molecular allotrope of carbon and consists of pentagonal and hexagonal rings as the basis of icosahedral symmetry closed cage structure [19]. Carbon nanotubes (CNTs) are cylindrical large molecules made of rolled-up sheets of single layer carbon atoms with a hexagonal arrangement [20]. The single layer of carbon atoms arranged in a honeycomb lattice structure is named graphene. This first discovered two-dimensional (2D) atomic crystal [21, 22] is widely used in many fields including catalysis, energy storage, gas sorption, and water purification [23–27]. In recent years, numerous 2D carbon-based materials further than graphene have been theoretically predicted or experimentally synthesized [28–38]. For example, graphyne is a single layer of sp and sp2 bonded carbon atoms [37, 38]. There are a vast number of possible graphyne sheets including α, β, γ and (6-6-12) graphyne sheets [37–39]. The symmetry and arrangement of acetylenic linkage are different in these sheets. They attracted particular interest due to their various electronic and optical properties [37–42]. Recently, another allotrope of carbon with energy lower than β-graphyne was proposed [43]. This sheet known as T4,4,4-graphyne, is a semiconductor with a direct band gap, unlike pristine graphene. Hence, it can be considered as a promising

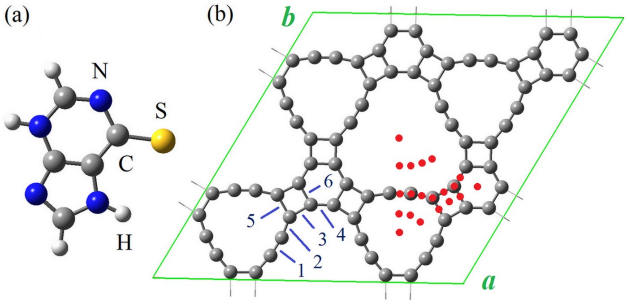

Figure 1. Atomic structure and of (a) mercaptopurine (MP) drug and (b) T4,4,4-graphyne sheet. The red dots show the possible sites on T4,4,4-graphyne sheet for MP adsorption.

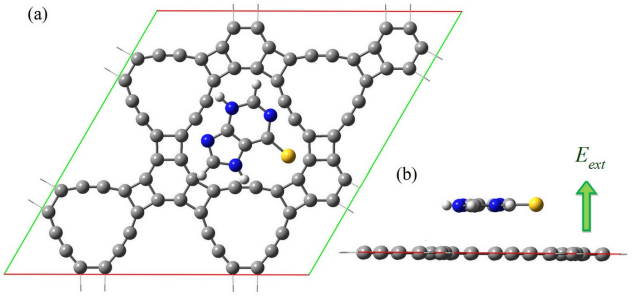

Figure 2. The most stable configuration of MP adsorbed on T4,4,4-graphyne sheet.

nanomaterial to use in future electronics. The gas sensing ability of T4,4,4-graphyne is examined. It is found that the electronic properties of T4,4,4-graphyne change with NO2, NO, CO2, and CO adsorption [44]. According to these results, we are motivated to study adsorption and detection of MP drug on T4,4,4-graphyne sheet through density functional theory (DFT) study.

2. Computational details

The DFT calculations are performed based on Perdew-Burke-Ernzerhof (PBE) parameterization of the generalized gradient approximation (GGA) [45] by using OpenMX3.8 code [46]. The DFT-D3 of Grimme is employed to import the effects of van der Waals (vdW) interactions [47]. The energy cutoff is considered to be 150 Ry for the wave-function expansions. The pseudo atomic orbital (PAO) formalism is used to describe the selection of the basis sets [48]. The PAO basis functions are specified by s2p2d1 (two s-state, two p-state, and one d-state radial functions) for C, N, S, and H atoms, within cutoff radii of basis functions set to the values of seven. Adsorption of MP (C5H4N4S) on a 2×2×1 supercell of T4,4,4-graphyne sheet consisting of 72 carbon atoms is studied. Atomic structures of MP drug and T4,4,4-graphyne sheet are displayed in Fig. 1. The lattice constant of the primitive unit cell of T4,4,4-graphyne sheet is 9.292$\AA$. A $2\times2\times1$ super cell is considered in a simulation box of a×b×c. The cell parameters are 18.584$\AA$ along the a and b axes. The c-axis is extended to 15$\AA$ to avoid interlayer interaction. The periodic boundary conditions are applied along with all space directions. All atomic structures are fully relaxed until the maximum force acting on each atom becomes less than $0.01eV/\AA$. The charge transfer between the sheet and molecule is gained utilizing Mulliken population analysis. The k-points for sampling over the Brillouin zone (BZ) integration are generated using the Monkhorst-Pack scheme [49]. For calculations of the electronic band structures, 21 k-points are considered along each high symmetry line in BZ.

To study the stability of T4,4,4-graphyne sheet and MP molecule, cohesive energy per atom is calculated by

$$E_{coh} = \frac{E_{sheet/MP} - \sum_i n_i E_i}{\sum_i n_i} \quad (1)$$

where,$E_{sheet/MP}$ denote the total energy of sheet or molecule. n_i and E_i are number and energy of atom (i=C, N, S, and H). Here, the negative cohesive energy indicates the structure is energetically stable.

To investigate MP adsorption on T4,4,4-graphyne sheet, the adsorption energy,E_{ads}, is determined by,

$$E_{ads} = \frac{E_{sheet+MP} - (E_{sheet} + nE_{MP})}{n} \quad (2)$$

where,$E_{sheet+MP}$,E_{sheet} , and E_{MP} are the total energies of T4,4,4-graphyne sheet in the presence of adsorbed MP, T4,4,4-graphyne sheet, and MP drug, respectively. The number of adsorbed molecules, n, increases from one to four in the present work. Based on equation 2, negative adsorption energy reveals the molecule adsorption is an exothermic process.

The enthalpy,H , is calculated using the following equation,

$$H = E + PV \quad (3)$$

here,E, is the total energy of system,P, denotes the applied pressure, and V is the volume of the cell.

3. Results and discussion

A supercell of T4,4,4-graphyne sheet with $2\times2\times1$ unit cells for adsorption of MP drug is shown in Fig. 1. The lengths of $C-C$ bonds (1 to 6 in Fig. 1) are 1.26, 1.33, 1.51, 1.38, 1.46, and 1.47$\AA$, respectively. Our calculated cohesive energy for T4,4,4-graphyne sheet is $-8.45eV/atom$, which is in good agreement with the past study [43]. The cohesive energy for T4,4,4-graphyne is comparable to that of γ-graphdiyne and much lower than that of β-graphdiyne [43]. This confirms the energetic favorability of T4,4,4-graphyne sheet and promises its realization in the future. The thermal and dynamical stabilities of T4,4,4-graphyne sheet are also reported previously [43]. The cohesive energy of MP drug is also calculated. The negative ($-6.87eV/atom$) denotes the formation of MP molecule is an exothermic process and its structure is stable.

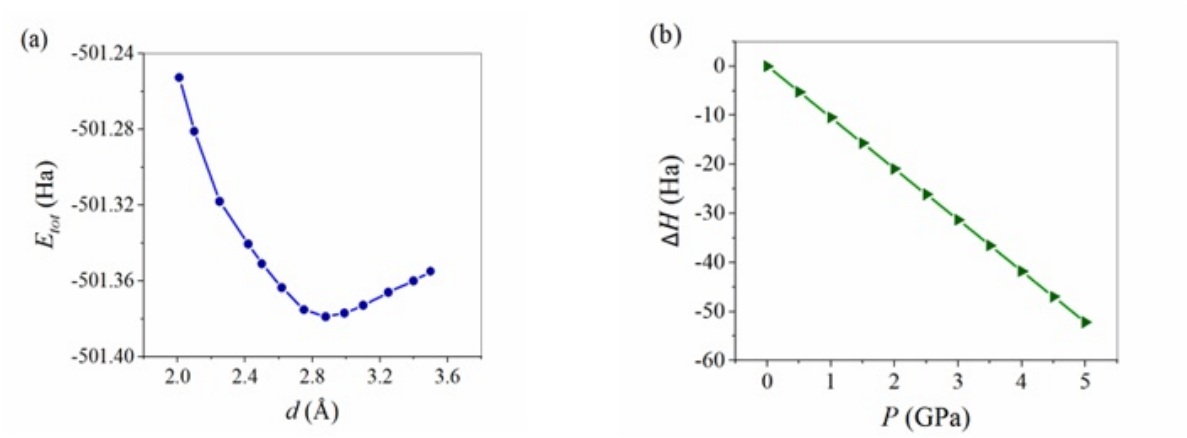

Figure 3. (a) Total energy, $E_{sheet+MP}$, as a function of adsorption distance, d, and (b) formation enthalpy, ΔH, as a function of adsorption distance, P, for MP adsorbed on T4,4,4-graphyne sheet.

To find the proper adsorption configuration, various adsorption sites are examined. In Fig. 1, twenty possible sites on T4,4,4-graphyne sheet for MP adsorption are illustrated by red dots. At each site, the orientation of the molecule on the sheet is changed and the total energy of the configuration is calculated. The configuration with the most negative energy is considered the most energetically favorable configuration. The most stable configuration of T4,4,4-graphyne sheet with MP adsorbed is shown in Fig. 2. It is observed that MP drug is preferably adsorbed parallel to the layer on top of the hollow site of the sheet. The distance between the adsorbed molecule and the sheet gradually increases from 2 to 3.5$\AA$ to determine the optimal distance. The total energy, $E_{sheet+MP}$, via the adsorption distance, d, is plotted in Fig. 3a. Here, the optimal adsorption distance and adsorption energy of the most stable structure are 2.88$\AA$ and $-0.69eV$, respectively. The large adsorption distance and small adsorption energy specify physisorption of MP drug on T4,4,4-graphyne sheet. The charge transfer between the adsorbed MP drug and the T4,4,4-graphyne sheet is studied to further investigate the interaction between the molecule and sheet. It is found that MP drug gains 0.016 e from the sheet. The C atoms of the MP drug lose electrons, while its N and S atoms gain electrons. This is because C atom is less electronegative than N and S atoms. This small charge transfer is also confirms MP drug interacts with T4,4,4-graphyne sheet through the weak physical adsorption.

The formation enthalpy, ΔH, from 0 to 50 GPa is calculated as the difference in the enthalpy of the system with respect to the isolated sheet and molecule. The formation enthalpy as a function of pressure is depicted in Fig. 3b. The negative formation enthalpies indicate that T4,4,4-graphyne sheet with adsorbed MP is thermodynamically stable under pressure.

To study the effect of MP drug on the electronic properties of T4,4,4-graphyne sheet, the electronic band structures and density of states (DOS) of the sheet before and after MP adsorption are determined. The electronic band structure and DOS of T4,4,4-graphyne sheet are shown in Fig. 4. It is found that T4,4,4-graphyne sheet is a direct band gap semiconductor. The energy band gap of $0.47eV$ is determined by using GGA-PBE. The band gap is evaluated 0.34 (GGA) and $0.63eV$ (HSE06) in the previous study [35]. The electronic band structure and DOS of T4,4,4-graphyne sheet with adsorbed MP are presented in Fig. 5. Adsorption of MP drug has no remarkable influence on both valence and conduction bands of T4,4,4-graphyne sheet. The state and DOS peak about $0.2eV$ below the Fermi level are induced by MP adsorption. Hence, the band gap reduces from 0.47 to $0.37eV$ in the presence of MP drug. To gain more insight into the effect of MP drug on the electronic properties of T4,4,4-graphyne sheet, partial DOS (pDOS) of T4,4,4-graphyne sheet with adsorbed MP is also plotted in Fig. 5. Here, pDOS illustrates the atomic contributions o to valence and conduction bands around the Fermi level. From pDOS, it is found that the occupied state and sharp DOS peak below the Fermi level are composed of C and S atoms of MP drug. Analysis of the pDOS showed that the contributions from the p_z orbitals of S and N are much higher than that from s, p_x, and p_y orbitals of these atoms.

It is reported that external electric fields can have significant effects on the electronic properties of 2D materials which play a crucial role in specifying their performance as gas sensors. Hence, the effects of the applied electric field on the adsorption energy, charge transfer, and energy band gap are investigated. Fig. 2 gives the schematic image of the electric field, which is perpendicular to the sheet with the positive (negative) direction aligned upward (downward). The variation of adsorption energy as a function of the electric field

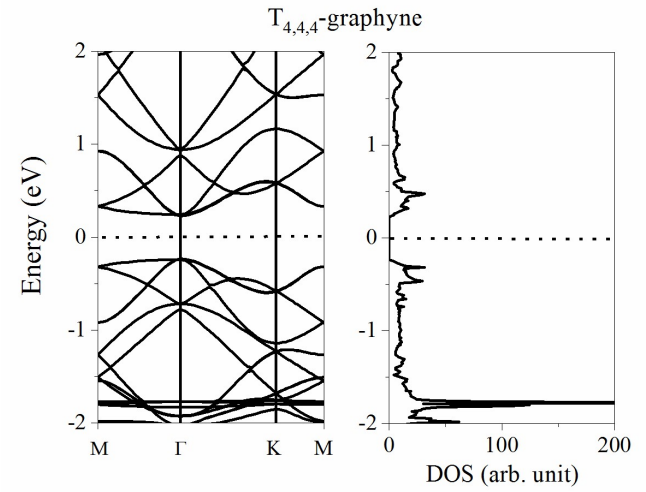

Figure 4. Electronic band structure and DOS of T4,4,4-graphyne sheet. (The Fermi level is set to $0eV$.)

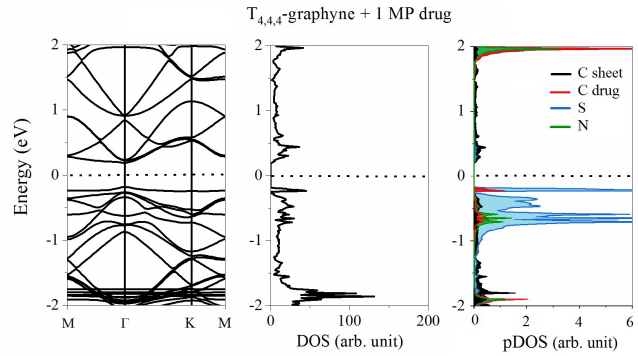

Figure 5. Electronic band structure, DOS, and pDOS of T4,4,4-graphyne sheet with adsorbed MP.

in the range of -1.0 to $1.0V/\AA$ is displayed in Fig. 6a. The adsorption energy becomes more negative (its absolute value increases) with applying a positive electric field. The adsorption energy significantly increases to $-14.7eV$ with applying an electric field of $+1.0V/\AA$ (Fig. 6a). This enhancement suggests that a positive electric field may improve the sensing ability of T4,4,4-graphyne sheet for MP detection. In contrast, the positive adsorption energy reveals that the structure becomes unstable when a negative electric field is applied. Hence, a negative electric field can be used for desorption of MP drug from the sheet.

The charge transfer as a function of the applied electric field is shown in Fig. 6b. Here, the positive ΔQ shows charge transferring from the MP drug to the sheet. It means the positive electric field of more than $0.05V/\AA$ leads to a charge transfer from MP drug to T4,4,4-graphyne sheet. The results show that the transferred charge is directly related to the binding strength. A positive electric field remarkably enhances the charge transfer between the molecule and sheet and causes strong chemical MP adsorption on the sheet.

It should be noted that more charge transfer between MP drug

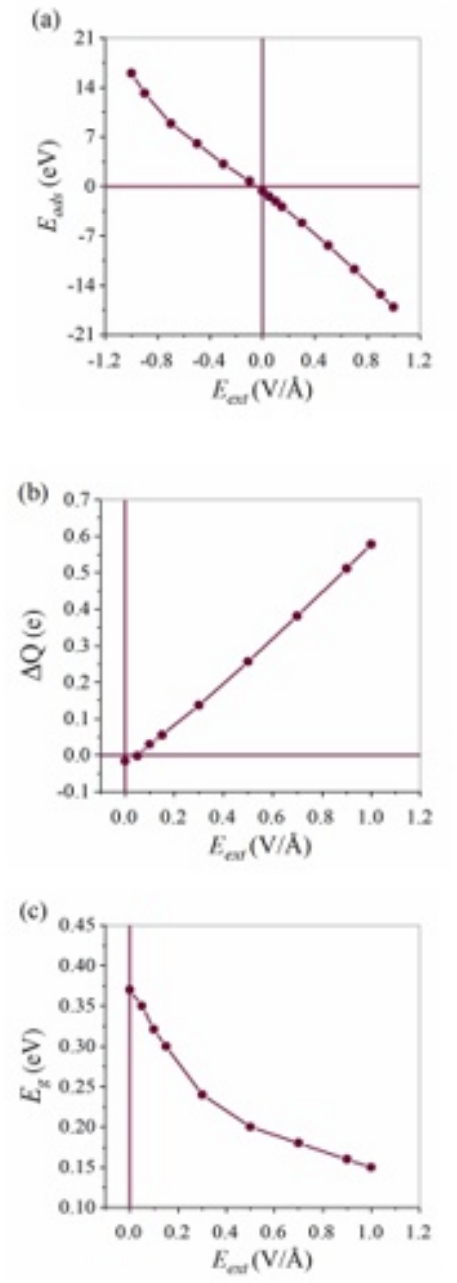

Figure 6. (a) Adsorption energy, E_{ads}, (b) charge transfer, ΔQ, and (c) energy band gap, E_g, as a function of the applied electric field, E_{ext} .

and T4,4,4-graphyne sheet could lead to remarkable changes in the electronic features of the sheet and consequently to the higher sensitivity of system as MP sensor. To explain the effect of electric field on the electronic properties, the electronic band structures as well as DOS of T4,4,4-graphyne sheet with adsorbed MP in the presence of electric field are calculated. For instance, the electronic band structure and DOS of T4,4,4-graphyne sheet with adsorbed MP under a positive electric

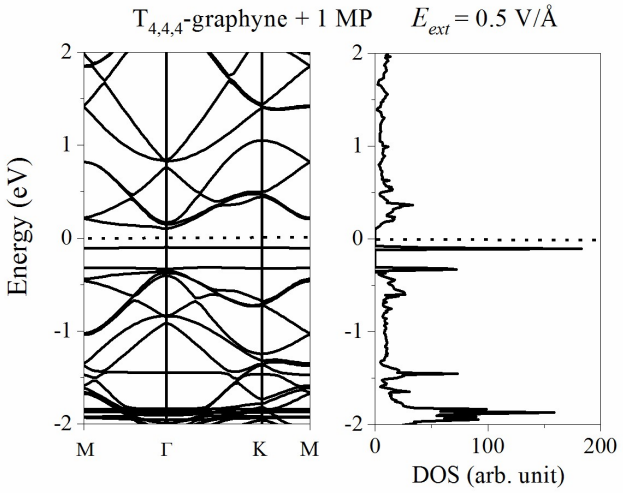

Figure 7. Electronic band structure and DOS of T4,4,4-graphyne sheet with adsorbed MP in the presence of an external electric field of $+0.5V/Å$.

field of $+0.5V/Å$ are plotted in Fig. 7. The impurity state shifts upwards to the Fermi level and causes decreasing the gap between the highest occupied and the lowest unoccupied states. The variation of the energy band gap with the electric field is illustrated in Fig. 6c. The energy band gap gradually decreases with enhancing the strength of the positive electric field.

We have focused on two to four MP molecules adsorbed on T4,4,4-graphyne sheet to study the sensitivity of the electronic properties of the sheet to the concentration of MP drug. As an example, the atomic structure of T4,4,4-graphyne sheet with three adsorbed MP molecules is displayed in Fig. 8a. The results indicate that MP molecules are physically adsorbed on the sheet with an adsorption energy of about $-0.65eV/molecule$. It is also found that there is $0.02e/molecule$ transferred from the MP drug to the sheet. In Fig. 8b, the electronic band structure of T4,4,4-graphyne sheet with three adsorbed MP is plotted. Similar to the results of mono-adsorbed MP, adsorption of two, three, and four MP molecules decrease the energy band gap to 0.30, 0.28, $0.27eV$, respectively. It is because the number of flat bands below the Fermi level increases with enhancing the number of MP molecules. Hence, the concentration of MP drug has a sizeable effect on the electronic properties of T4,4,4-graphyne sheet.

4. Conclusions

We have studied MP adsorption on T4,4,4-graphyne sheet using DFT. The most stable adsorption structure, adsorption energy, and charge transfer are obtained. It is shown that the MP drug is weakly physisorbed on the sheet and gains electrons from the sheet. The electronic band structures, as well as DOS, show that T4,4,4-graphyne sheet is a semiconductor with an intrinsic energy band gap. The energy band gap

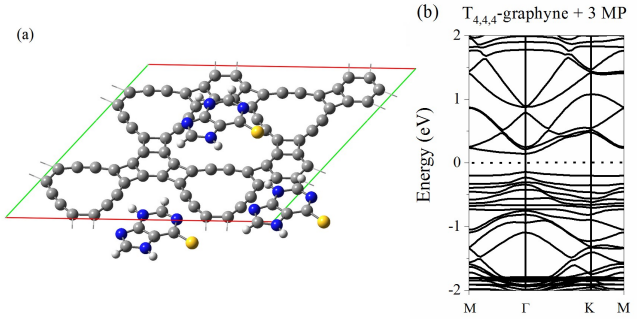

Figure 8. (a) Atomic structure and (b) electronic band structure of T4,4,4-graphyne sheet with three adsorbed MP.

reduces with the adsorption of MP drug. This finding shows that T4,4,4-graphyne sheet has great potential to fabricate sensors for MP detection. It is also demonstrated that applying a perpendicular electric field can change the charge transfer between MP and the sheet, and affect the energy band gap. A positive electric field enhances the adsorption of MP on T4,4,4-graphyne sheet as reflected in the enhancement of adsorption energy. In contrast, the interaction becomes weaker under a negative electric field. Hence, a negative electric field could be applied for MP desorption. The sensitivity of the electronic properties of T4,4,4-graphyne sheet to the concentration of MP drug is also studied. It is shown that the energy band gap decreases by enhancing the number of adsorbed molecules. Our results showed that the electronic properties of T4,4,4-graphyne sheet have high sensitivity to MP drug and its concentration. The higher sensitivity of T4,4,4-graphyne sheet to the MP could be realized with the help of an extra electric field.

References

[1] Y. Yang, A. Sun, and W. Gu. *Struct. Chem.*, **32**:457, 2021.

[2] L. Wang and Z. Zhang. *Talanta.*, **76**:768, 2008.

[3] M. Keyvanfard, V. Khosravi, H. Karimi-Maleh, KH. Alizad, and B. Rezaei. *J. Mol. Liq.*, **177**:182, 2017.

[4] B. Norgard, L. Pedersen, K. Fonager, S. Rasmussen, and H. Sorensen. *Aliment. Pharm. Ther.*, **17**:827, 2013.

[5] A. Dignass, G. Van Assche, J.O. Lindsay, M. Lémann, J. Söderholm, J.F. Colombel, S. Danese, A.D'. Hoore, M. Gassull, F. Gomollón, D.W. Hommes, P. Michetti, C. O'Morain, T. Öresland, A. Windsor, E.F. Stange, S.P.L. Travis, European Crohn's, and Colitis Organisation (ECCO). *Nucl. Instruments Methods Phys. Res. Sect. A Accel. Spectrometers, Detect. Assoc. Equip.*, **4**:63, 2010.

[6] J. Bo, H. Schroder, J. Kristinsson, B. Madsen, C. Szumlanski, R. Weinshilboum, J.B. Andersen, and K. Schmiegelow. *J. Theor. Appl. Phys.*, **86**:1080, 1999.

[7] L. Wang and Z. Zhang. *Talanta.*, **76**:768, 2008.

[8] R. Boulieu and T. Dervieux. *J. B Biomed. Sci. Appl.*, **730**:273, 1999.

[9] C.C. Wang, S.S. Chiou, and S.M. Wu. *Electrophoresis*, **26**:2639, 2005.

[10] T. Dervieux and R. Boulieu. *Clin. Chem.*, **44**:551, 1998.

[11] A.A. Ensafi and H. Karimi-Maleh. *Drug Test Anal.*, **4**:970, 2012.

[12] V. Vahabi and H. Soleymanabadi. *J. Mex. Chem.*, **60**:34, 2016.

[13] M. Li Y. Wei, G. Zhang, F. Wang, M. Li, and H. Soleymanabadi. *Physica E*, **118**:113878, 2020.

[14] R. Majidi and M. Nadafan. *Phys. Lett. A*, **384**:126036, 2020.

[15] Y. Wang and T.W. Yeow. *J. Sensors*, **2009**:493904, 2009.

[16] E. Llobet. *Sens. Actuators B, Chem.*, **179**:32, 2013.

[17] R. Majidi and A.R. Karami. *Indian J. Phys.*, **88**:483, 2014.

[18] M. Fouladgar, H. Karimi-Maleh, F. Opoku, and P. Poomani Govender. *J. Mol. Liq.*, **311**:113314, 2020.

[19] P.A. Troshin and R.N. Lyubovskaya. *Russ. Chem. Rev.*, **77**:323, 2008.

[20] S. Iijima. *Nature*, **354**:56, 1991.

[21] K. S. Novoselov. *Science*, **306**:666, 2004.

[22] K.S. Novoselov, A.K. Geim, S.V. Morozov, D. Jiang, M.I. Katsnelson, I.V. Grigorieva, S.V. Dubonos, and A.A. Firsov. *Nature*, **438**:197, 2005.

[23] M. Mirzaei and R. Salamat Ahangari. *Int. J. Nano Dimens.*, **7**:284, 2016.

[24] M. Corosm, F. Pogacean, L. Magerusan, C. Socaci, and S. Pruneanu. *Front. Mater. Sci.*, **13**:23, 2019.

[25] S. Ren, P. Rong, and Q. Yu. *Ceram. Int.*, **44**:11940, 2018.

[26] V. Tozzini and V. Pellegrini. *Phys. Chem. Chem. Phys.*, **15**:80, 2013.

[27] H. Beitollai, M. Safaei, and S. Tajik. *Int. J. Nano Dimens.*, **10**:125, 2019.

[28] Y. Lin, Q. Huang, L. Guo, and X. Chen. *Phys. Rev. Lett.*, **108**:225505, 2012.

[29] J.W. Yin, E.Y. Xie, M.L. Liu, R.Z. Wang, X.L. Wei, L. Lau, J.X. Zhong, and Y.P. Chen. *J. Mater. Chem.*, **1**:5341, 2013.

[30] J. Mahmood, E. Kwang Lee, M. Jung, D. Shin, I. Jeon, S.M. Jung, H.J. Choi, J.M. Seo, S.Y. Bae, S.D. Sohn, N. Park, J.H. Oh, H.J. Shin, and J.B. Baek. *Nat. Commun.*, **6**:6486, 2015.

[31] M. Yagmurcukardes, S. Horzum, E. Torun, F.M. Peeters, and R. Tugrul Senge. *Phys. Chem. Chem. Phys.*, **18**:3144, 2016.

[32] N.V.R. Nulakani and V. Subramanian. *J. Phys. Chem. C*, **120**:15153, 2016.

[33] R. Majidi. *Can. J. Phys.*, **94**:305, 2016.

[34] R. Majidi. *Physica E*, **90**:189, 2017.

[35] R.M. Tromer, M.G.E. da Luz, M.S. Ferreira, and L.F.C. Pereira. *J. Phys. Chem.*, **121**:3055, 2017.

[36] R. Majidi. *Theor. Chem. Accounts*, **136**:109, 2017.

[37] B.G. Kim and H.J. Choi. *Phys. Rev. B*, **86**:115435, 2012.

[38] D. Malko, C. Neiss, F. Vines, and A. Gorling. *Phys. Rev. Lett.*, **108**:086804, 2012.

[39] J. Kang, Z. Wei, and J. Li. *ACS Appl. Mater. Interfaces*, **11**:2692, 2019.

[40] B. Bhattacharya, J. Deb, and U. Sarkar. *AIP Adv.*, **9**:095031, 2019.

[41] R. Majidi and A.R. Karami. *Mol. Phys.*, **11**:3194, 2013.

[42] B.Bhattacharya, U. Sarkar, and N. Seriani. *J. Phys. Chem. C*, **120**:26579, 2016.

[43] W. Wanga, L. Li, X. Kong, B. Van Duppen, and F.M. Peeters. *Solid State Commun.*, **293**:23, 2019.

[44] R. Majidi and u. Sarkar. *Mol. Simulat.*, **46**:1383, 2020.

[45] J.P. Perdew, K. Burke, and M. Ernzerhof. *Phys. Rev. Lett.*, **77**:3865, 1996.

[46] T. Ozaki, H. Kino, J. Yu, M.J. Han, N. Kobayashi, M. Ohfuti, F. Ishii, and et al. *User's manual of OpenMX Ver. 3.8*. OpenMX, 2017.

[47] S.J. Grimme. *Comput. Chem.*, **27**:1787, 2006.

[48] T. Ozaki and H. Kino. *Phys. Rev. B.*, **69**:195113, 2004.

[49] H.J. Monkhorst and J.D. Pack. *Phys. Rev. B*, **13**:5188, 1976.